

Cite this: *Mater. Adv.*, 2026,  
7, 1918

# The role of bio-based constituents in additive manufacturing with thermosetting polymers and vitrimers: a review

Eliott Bonnet Martin,<sup>ab</sup> Aurore Denneulin,<sup>a</sup> Michael Lecourt,<sup>b</sup> Mark Irle<sup>b</sup> and Davide Beneventi<sup>a</sup>

This review focuses on the additive manufacturing of thermoset polymers incorporating at least one bio-based constituent, whether as a filler or as the thermoset polymer itself. In this work, bio-based thermosets reviewed are mostly epoxy, acrylate, methacrylate and thiol-ene resins. The micro-scale fillers developed in additive manufacturing mainly source from woody biomass, with wood particles but also cellulose powder and lignin. Nano-scale fillers use is also reported with cellulose nano crystals, chitin nano crystals and carbon dots derived from cellulose. Additive manufacturing was chosen as the focus due to its broad range of applications and significant sustainability advantages, including reduced waste, shorter value chains, and easier repairability. Furthermore, the growing demand for bio-based polymers is driven by the anticipated shortage of fossil-based alternatives. This review demonstrates the relevance of this timely topic and highlights the extensive research efforts dedicated to bio-based thermosets and thermosets with bio-based fillers, showcasing a diverse array of innovative approaches explored across 83 studies. Overall, despite significant progress in the development of bio-based thermosets, the dependence on petroleum-derived photoinitiators, together with the limited understanding and control of curing kinetics and rheological behavior of neat and composite precursors, remain major challenges that must be addressed to enable the industrial scale-up of these additive manufacturing materials.

Received 4th June 2025,  
Accepted 20th November 2025

DOI: 10.1039/d5ma00585j

rsc.li/materials-advances

## 1. Introduction

Additive manufacturing (AM) is a rapidly advancing technology that constructs objects layer by layer from computer-generated designs.<sup>1</sup> Compared to conventional manufacturing methods, AM is widely regarded as a more environmentally sustainable approach,<sup>2</sup> as it reduces energy consumption, shortens processing times, and minimizes material waste.<sup>2,3</sup> Thermoplastics are predominant in AM because they can be melted multiple times making them easier to handle.<sup>1</sup> Thermosets, on the other hand, keep their shape when heated. Difference in behavior is explained by the differences in the chemical structures between thermosets and thermoplastics, thermoplastics are linear polymers while thermosets are crosslinked in three dimensions.<sup>2</sup> This offers thermosets superior heat and chemical resistance.<sup>3</sup>

Additionally, they can be more rigid and durable once cured, making them suitable for a wide range of applications where strength and longevity are crucial.<sup>4</sup> The incorporation of bio-based constituents in the formulation of thermoset inks for AM is a recent advancement that has the potential to make this technology more sustainable and truly revolutionize material manufacturing. Despite their attractive properties (Table 1), the major drawback of thermosets compared to thermoplastics lies in their lack of recyclability, which exacerbates the environmental impact of petroleum-derived thermosets and restricts their use to niche applications. Substituting petrosourced oligomers with bio-based alternatives may offer a viable

Table 1 Comparison of key properties between thermoplastics and thermosets

Thermoplastics	Thermosets
Linear/branched chains	Crosslinked
Harden on freezing	Need curing
Limited heat resistance	Excellent thermal/chemical resistance
Tough and ductile	Brittle and rigid
Easily melted and recycled	Challenging recyclability

<sup>a</sup> Univ. Grenoble Alpes, CNRS, Grenoble INP (Institute of Engineering Univ. Grenoble Alpes), LGP2, Grenoble, France. E-mail: eliot.bonnet-martin1@grenoble-inp.fr, davide.beneventi@pagora.grenoble-inp.fr, aurore.denneulin@grenoble-inp.fr

<sup>b</sup> FCBA, Institut Technologique, Grenoble, France.

E-mail: Eliott.BONNETMARTIN@fcba.fr, Michael.LECOURT@fcba.fr, mark.irle@fcba.fr



strategy to reduce the environmental footprint of thermosets and broaden their applicability.

This review focuses on the use of bio-based compounds in the AM of thermosets, aiming to identify the challenges and opportunities for bio-based thermosets and bio-based fillers in AM by exploring the various reasons these compounds are of interest and how they are incorporated to meet AM requirements. The overview is divided into three parts describing (i) the different additive manufacturing techniques used for printing of bio-based thermosets and bio-composites, (ii) the thermosetting bio-polymers themselves and (iii) most widely used bio-based fillers.

## 2. Different manufacturing techniques

The two main technologies in bio-based AM are material extrusion techniques and vat photopolymerization. While a wide array of techniques can be qualified as AM, only a few of them have been used for the AM of partially bio-based thermosets, namely, stereolithography (SLA), digital light processing (DLP), liquid-crystal display AM (LCD), which are vat techniques, and liquid deposition modelling (LDM), which is an extrusion technique. Vat photopolymerization techniques are currently favored to the extrusion-based LDM, which is a newer and less mature technology, even though LDM shows very promising results for a wider range of materials.<sup>7</sup> Fig. 1 provides a schematic summary of the AM approaches considered for bio-based thermosets. Whether it is extrusion-based

AM or VAT photopolymerization the additive manufacturing process workflow is the same for synthetic and bio-based resins, only parameters such as layer thickness or curing time can vary because of differences in curing kinetics for each resin.

### 2.1. Vat photopolymerization

Vat photopolymerization relies on locally triggering the polymerization of a liquid photosensitive resin using a light source. This resin is a blend of oligomers and monomers with a photoinitiator (*i.e.* a molecule that absorbs UV or visible light and converts the photonic energy into reactive species, either radicals or cations, thereby initiating the photopolymerization reaction<sup>8</sup>).

The object is formed layer by layer on the printing platform by progressively curing the liquid resin located in a bath. The object is either formed by top-down or bottom-up polymerization. In top-down polymerization each layer is cured at the surface of the bath with the light source placed above the bath and the platform lowering progressively. In bottom-up polymerization the light source is placed below the bath and the bottom of the bath is cured first while raising the platform.<sup>9</sup> This approach requires a transparent vat bottom to allow the light to pass through and initiate the polymerization process. Curing the surface of the bath eases the accessibility of the light source but requires a larger volume of liquid resin, because the platform is lowered until the printed object is completed, and, consequently, the depth of the resin bath must be larger than the object being printed.

**2.1.1. Stereolithography (SLA).** The invention of stereolithography is attributed to Chuck Hull in 1986.<sup>10</sup> In SLA, the

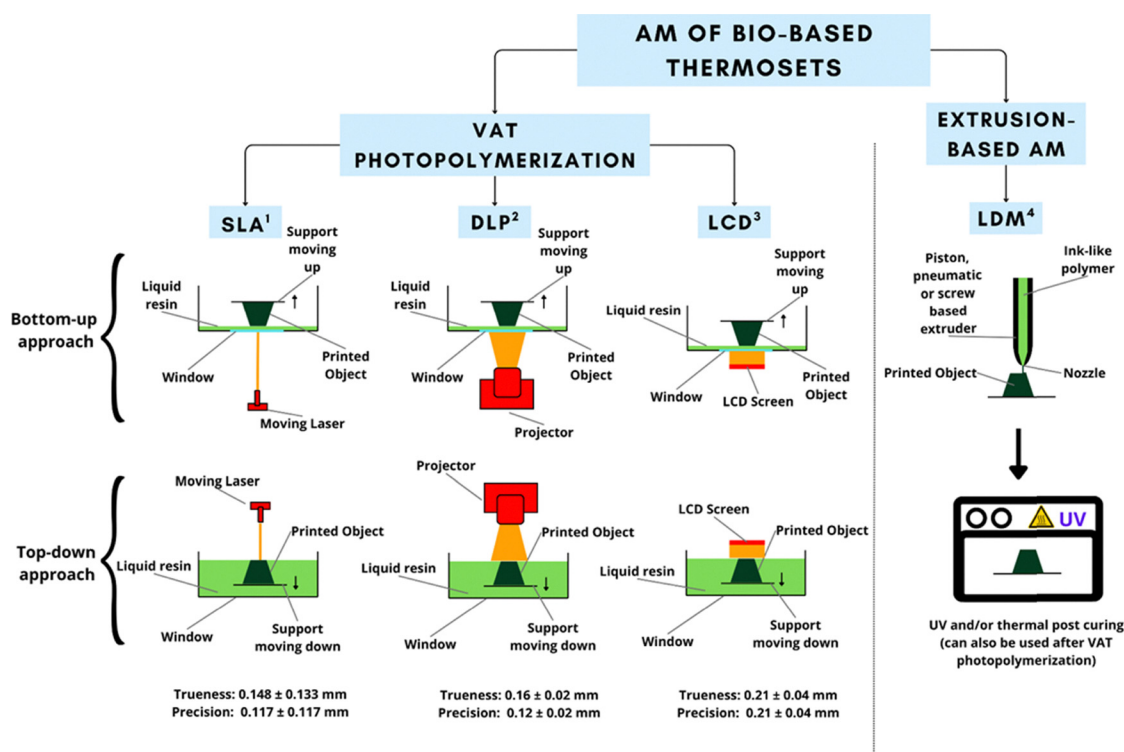


Fig. 1 Schematic representation of the different additive manufacturing techniques currently used for bio-based thermosets.<sup>1</sup> SLA: stereolithography,<sup>2</sup> DLP: digital light processing,<sup>3</sup> LCD: liquid-crystal display,<sup>4</sup> LDM: liquid deposition modelling.



light source is a laser moving to create a pattern for each layer. For this reason, it is the most time-consuming vat photopolymerization technique, but it has a good precision with a layer height between 12 and 150  $\mu\text{m}$ .<sup>11,12</sup> The incorporation of bio-based photopolymers or bio-fillers does not change the way SLA and other vat photopolymerization operates, which could help achieving the replacement of petroleum-based materials more easily.

**2.1.2. Digital light processing (DLP).** The main difference between DLP and SLA lies in the light source used to cure the resin. In DLP, the moving laser of SLA is replaced by a digital light projector.<sup>9</sup> Instead of tracing the pattern layer by layer with a moving light source, the digital projector flashes the whole pattern at once.<sup>9</sup> This allows faster print times than SLA but could also affect the shape of the printed objects due to the inherent resolution of each systems.<sup>9,12</sup> Indeed, since DLP projects pixelated images, the parts produced with DLP will be voxelated, leading to a grainier result especially on curved surfaces.<sup>12</sup> In addition, the laser used in SLA is a round dot which means the printed part will be smoother.

**2.1.3. Liquid crystal display (LCD).** Liquid crystal displays are constituted of a backlight and a liquid crystal layer.<sup>13</sup> These liquid crystals can modify or block the backlight when an electric field is applied to them, allowing to create patterns.<sup>11</sup> LCD additive manufacturing is one of the most recent additive manufacturing techniques, it is similar to DLP as for each layer it projects the pattern for one layer at once, it also inherits the same voxelation issues as DLP. LCD machines are cheap, but

their lifespans are shorter than DLP and SLA because the light source is closer to the resin bath which means it receives a part of the heat from the curing reaction which can cause damage to the display, additionally UV light can also damage the liquid crystals.<sup>11,14</sup> The precision and the trueness of LCD additive manufacturing machines were also lower: standard deviations for precision is  $0.21 \pm 0.04$  mm for LCD compared to  $0.12 \pm 0.02$  mm for DLP and for trueness  $0.21 \pm 0.04$  mm for LCD compared to  $0.16 \pm 0.02$  mm for DLP.<sup>15</sup>

## 2.2. Extrusion-based additive manufacturing

Extrusion-based AM encompasses different layer by layer deposition techniques done by extruding a polymer through a nozzle. Fused filament fabrication (FFF) is the most widespread extrusion based additive manufacturing technique.<sup>16</sup> In FFF, a solid filament is fed to the printer and heated up until melted and is then extruded at a precise location to produce the desired shape.<sup>9</sup> It solidifies again on freezing. It is not adapted to thermosetting polymers because there is a risk that the thermoset crosslinks when producing self-standing filaments, this crosslinking would irreversibly harden the polymer making it impossible to melt it in the hot end of FFF hot end. In contrast, during liquid deposition modelling (LDM) the material is in liquid form and is hardened after the extrusion which makes it the only extrusion-based additive manufacturing technique currently existing for bio-based thermosets or bio-composites. Liquid deposition modelling is sometimes referred to as Direct Ink Write (DIW) (Fig. 2).

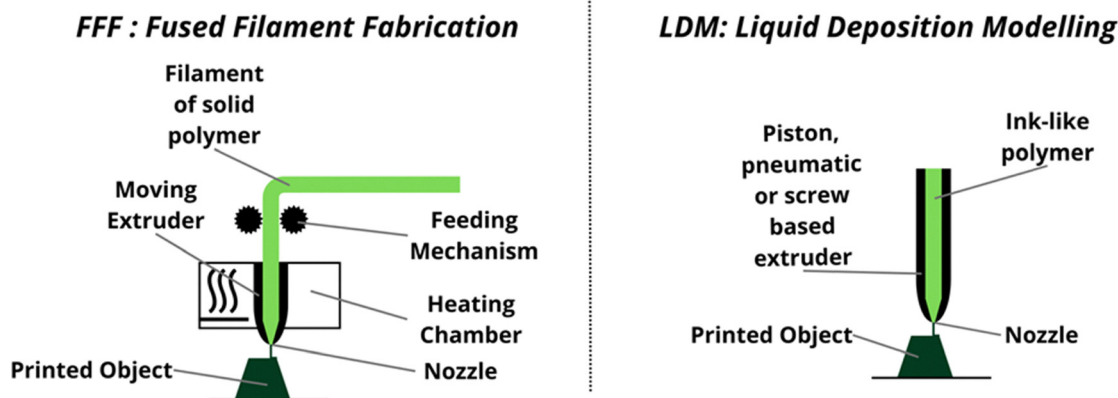


Fig. 2 Schematic representation of extrusion based additive manufacturing techniques.

Table 2 Advantages and disadvantages of additive manufacturing techniques for bio-based thermosets

	SLA	DLP	LCD	LDM
Printable polymers	Only photopolymers	Only photopolymers	Only photopolymers	Any thermoset
Printing resolution <sup>a</sup>	XY ~ 25–100 $\mu\text{m}$ Z ~ 25–100 $\mu\text{m}$	XY ~ 30–100 $\mu\text{m}$ Z ~ 25–100 $\mu\text{m}$	XY ~ 35–75 $\mu\text{m}$ Z ~ 25–100 $\mu\text{m}$	XY ~ 100–1000 $\mu\text{m}$ Z ~ 100–1000 $\mu\text{m}$
Surface aspect	Smooth	Voxelated	Voxelated	Textured
Printing time	++	+++	+++	+
Post-curing	Optional	Optional	Optional	Required
Scalability	++	+++	++	+
Equipment cost	€€€	€€€	€	€
Equipment service life	++	++	+	+++

<sup>a</sup> Can vary depending on printer and resin type.



The three main types of extrusion systems used in LDM are: (i) syringe-based extrusion, where the liquid is directly pushed through the nozzle by the movement of a syringe; (ii) pneumatic extrusion, which operates on the same principle but uses compressed air to force the liquid through the nozzle; and (iii) screw-driven extrusion, where a rotating screw drives the liquid through the nozzle.<sup>17</sup> Right after extrusion, the liquid is cured either by heating<sup>18</sup> or UV exposure<sup>19</sup> on the printing platform to maintain the desired shape (Table 2).

Novel additive manufacturing techniques such as delayed extrusion of cold masterbatch (DECMA) are optimized for the manufacturing of thermosets especially bio-based.<sup>20</sup> In this technique, the viscosity and the temperature are controlled to increase the printability of the materials. DECMA has been used to print a bioepoxy resin that was not printable with direct extrusion, this technique opens opportunities in additive manufacturing to a wider range of bio-based thermosets. DECMA is not industrially scalable yet because the printing requires 30 minutes of processing times for each layer while direct extrusion only takes a few seconds making a print take up to 2.5 hours. For this reason, despite the potential of DECMA it has only been reported in one work and efforts to improve the processing time and scalability of the technique are not currently investigated.<sup>20</sup>

### 3. Thermosetting biopolymers for AM

A wide variety of thermosetting biopolymers can be used for additive manufacturing. However, they often present the same key functional groups namely, epoxy, acrylate, methacrylate and thiol-alkene. The properties of the final products, the bio-based platforms and the curing kinetics of each of these systems will be discussed in this review. Knowledge of curing kinetics is essential to determine key parameters such as curing time, printing speed or intensity of the light sources, to produce prints with high trueness and good layer adhesion.<sup>21</sup>

On a side note, some of the polymers presented are not thermosets but vitrimers, they are similar to thermosets in the sense they also have a cross-linked network, but this cross-linking is reversible unlike thermosets. Consequently, vitrimers can be recycled more easily.<sup>22</sup> They can be as mechanically

resilient as thermosets and they are included in this study for this reason.<sup>23</sup>

#### 3.1. Epoxy-based resins

Epoxy resins are commonly used for the formulation of thermosetting polymers and bio-based synthesis routes are widely investigated.<sup>24</sup> These thermosets benefit from excellent mechanical strength and toughness as well as other interesting properties such as excellent chemical and moisture stability and good thermal, adhesive and electrical properties, making them suitable for a variety of applications. The polymerization reaction occurs between an epoxy and a compound containing two active hydrogen atoms often from hydroxy groups (Fig. 3).<sup>25</sup>

Multiple different bio-based constituents can be epoxidized to create bio-epoxy resins. The main bio-based raw materials used to produce bio-epoxy are vegetable oils,<sup>26–28</sup> lignin,<sup>29–31</sup> furan and its derivatives,<sup>32–34</sup> sorbitol and its derivatives,<sup>35</sup> rosin,<sup>36,37</sup> tannin,<sup>38</sup> resorcinol<sup>34</sup> and cardanol.<sup>18</sup> Among these resins, vegetable oil-based ones are the most common in AM, largely because they are largely available and relatively inexpensive especially soybean oil with 45 million tons produced in 2013.<sup>39</sup> The main bio-based epoxy constituent is detailed in Fig. 4.

The Young's moduli for the bio-based epoxy resins reviewed range from 0.37 MPa to 3700 MPa. Resorcinol and furan can produce stiff materials (Table 3), however they have a black color and are completely opaque due to either the lignin filler or the resorcinol and furan dimethanol used in the formulation of the polymer (Fig. 5a–c).<sup>20,28</sup> This can cause several problems, the printed objects are limited in terms of esthetic choices, and the color can hinder the curing if it does not let the UV light go through the polymer. Vegetable oil and cardanol based resins also exhibit a strong opacity and a brown color in contrast to traditional, colorless and transparent, epoxy resins (Fig. 5d and e).<sup>18,34</sup> Vegetable oil-based resins have weaker Young's moduli as well as more visible layer lines (Fig. 5d), this is explained by the fact these resins are formulated with fillers which lower the cross-linking by interfering with the reaction.<sup>28</sup> Additionally, vegetable oils lack reactivity and have lower strength and stiffness because of their lack of aromatic and cycloaliphatic structure.<sup>42</sup> Cardanol based resin exhibits even larger layer

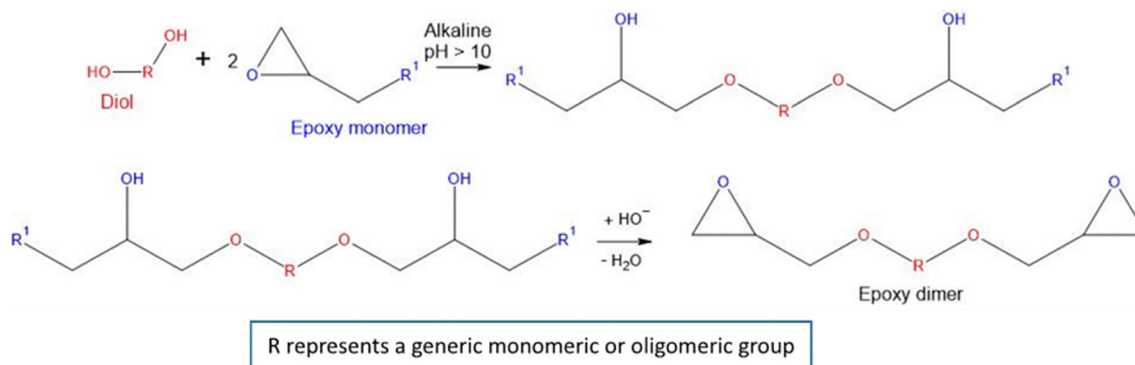


Fig. 3 Schematic representation of the dimerization reaction of epoxy resins.



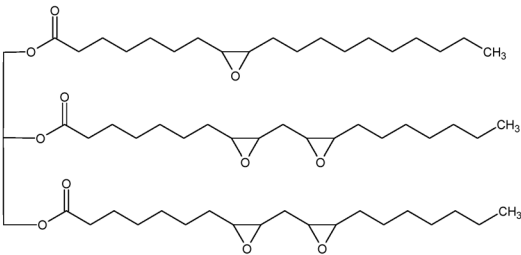
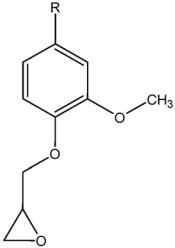
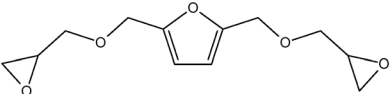
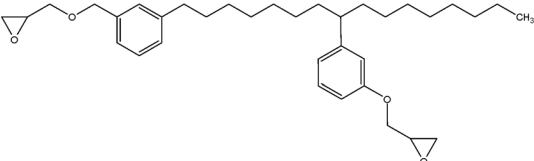
Chemical compound	Chemical structure of the epoxidized monomers	T <sub>g</sub> (°C)
Epoxidized vegetable oil		Soybean oil: between 58 and 67 °C Linseed oil: between 68 and 134 °C
Epoxidized lignin		With R the lignin polymer ~160 °C
Furandimethanol diglycidyl ether		Between 62 and 142 °C
Epoxidized cardanol		Between 15 and 19 °C

Fig. 4 Main bio-based epoxy systems.<sup>40,41</sup>

lines (Fig. 5e), however, this is due to the use of the technique LDM coupled with the high viscosity of the extruded resin.<sup>18</sup> Tuning the curing kinetics for additive manufacturing can be a challenge, especially for bio-based resins who tend to have slower kinetics, two approaches have been reported, increasing the curing temperature<sup>34</sup> or increase curing time.<sup>20</sup> The choice of the right photoinitiator is also shown to be of great importance, however, the motivation behind this choice is rarely reported, except in rare instances.<sup>28</sup>

### 3.2. Acrylate and methacrylate-based resins

Acrylate and methacrylate resins are thermosetting polymers with respectively acrylic acid and methacrylic acid as base monomers performing a radical polymerization reaction (Fig. 6). Similarly to epoxy resins, they exhibit very interesting properties: good mechanical strength, high glass transition temperature, thermal stability and transparency which can be particularly interesting in the context of a light activated reaction such as SLA.<sup>43</sup>

Bio-based substitutions for the acrylate or methacrylate monomers include lignin,<sup>44,45</sup> vanillin which is often also

derived from lignin,<sup>45–49</sup> vegetable oils,<sup>50–54</sup> eugenol,<sup>46,48,52</sup> guaiacol,<sup>46,48</sup> terpene<sup>55</sup> and lactic acid.<sup>56</sup>

The photoinitiators used with methacrylate and acrylate resins are petroleum based with a great majority using phenyl-bis(2,4,6-trimethylbenzoyl)-phosphine oxide (BAPO) and diphenyl (2,4,5-trimethylbenzoyl) phosphine oxide (TPO) which are also the most common in 3D printing of synthetic acrylate and methacrylate resins, these photoinitiators are petroleum based, they represent a small fraction of the polymer (less than 5% wt) but they show the reliance of bio-based resins on petroleum based compounds. While photoinitiator compatibility with the system can be a challenge especially with bio-based resins it has not been reported as an issue for acrylate and methacrylate additive manufacturing.

The tensile strength for acrylate and methacrylate resins range from 0.4 MPa to 55 MPa, even going up to 89 MPa for an epoxy methacrylate, on the higher end of this range the prints tensile strength is on par with what can be expected for commercial acrylate and methacrylate resins. The apparent downside of 3D printing of methacrylate and acrylate resins is that the commercially comparable results are obtained for



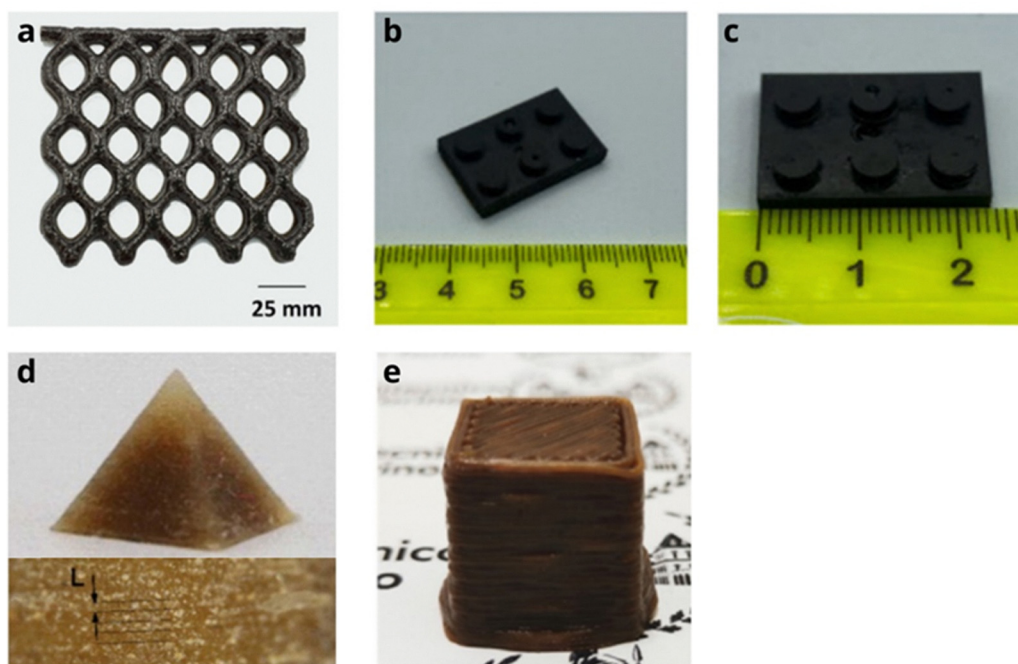


Fig. 5 (a) Commercial bio-epoxy resin print<sup>20</sup> (b) Resorcinol epoxy resin print Reproduced with permission from Elsevier, copyright 2022<sup>34</sup> (c) Furan dimethanol epoxy resin print Reproduced with permission from Elsevier, copyright 2022<sup>34</sup> (d) Linseed oil epoxy resin print and its optical analysis<sup>28</sup> (e) Cardanol epoxy resin print Reproduced with permission from Elsevier, copyright 2023.<sup>18</sup>

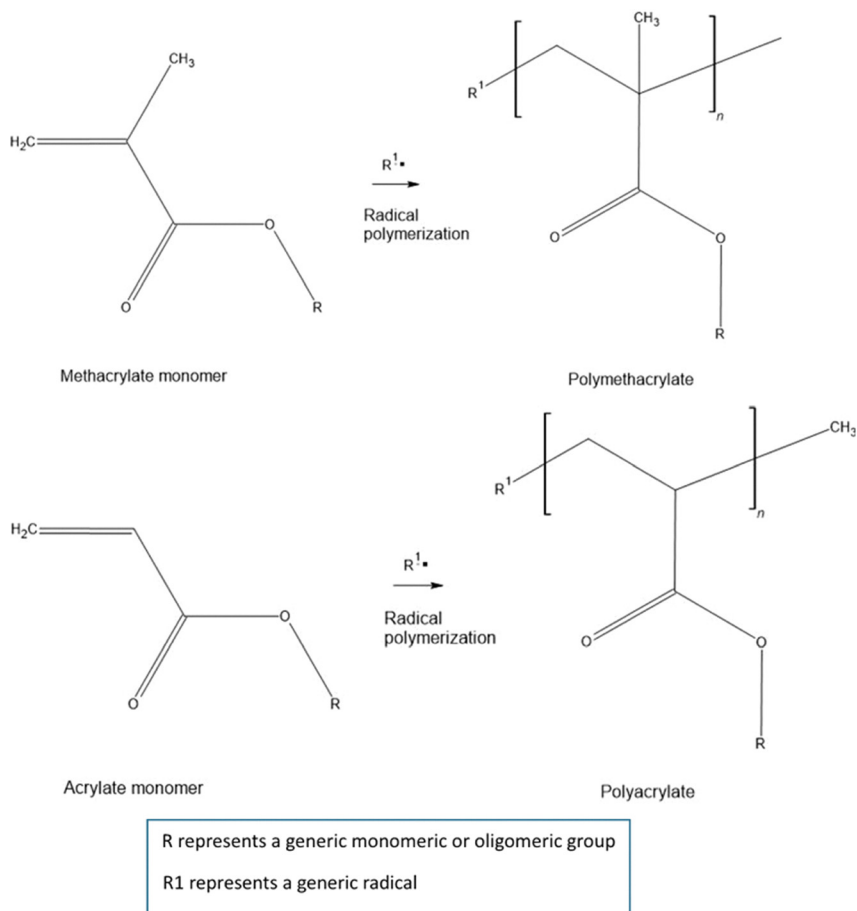


Fig. 6 Schematic representation of the polymerization reaction of acrylate and methacrylate resins.



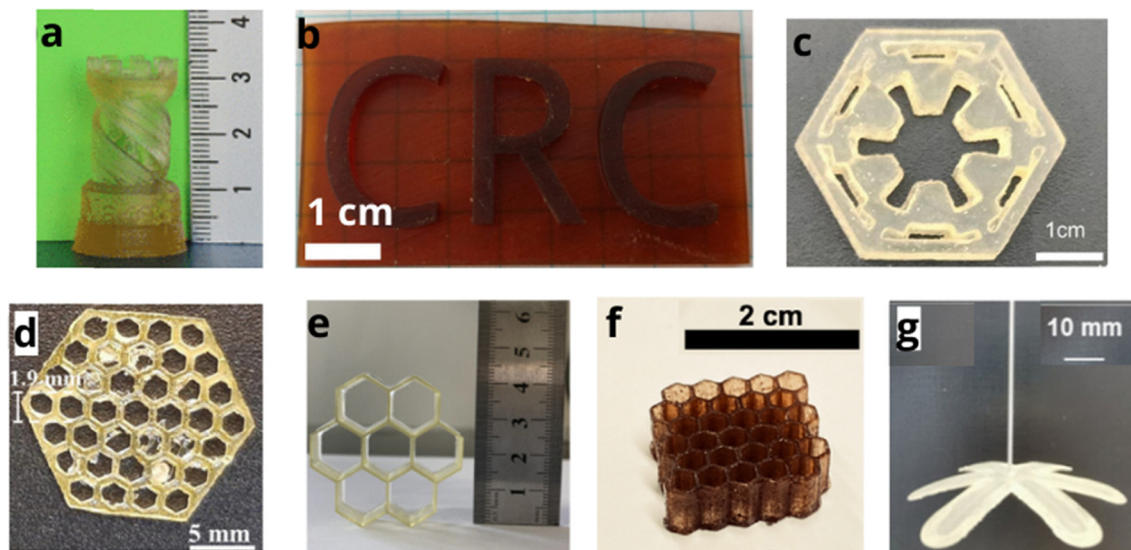


Fig. 7 (a) Soybean oil methacrylate resin print Reproduced with permission from American Chemical Society copyright 2020<sup>51</sup> (b) Lignin acrylate/methacrylate resin print Reproduced with permission from American Chemical Society, copyright 2018<sup>44</sup> (c) Palm oil methacrylate/acrylamide resin print Reproduced with permission from Elsevier, copyright 2023<sup>53</sup> (d) Vanillin methacrylate resin print<sup>49</sup> (e) Palm oil methacrylate/acrylate resin print Reproduced with permission from American Chemical Society, copyright 2023<sup>54</sup> (f) Vanillin, soybean oil and lignin methacrylate/acrylate resin print<sup>45</sup> (g) Glycerol acrylate and tetrahydrofurfuryl methacrylate resins print<sup>50</sup>

the prints with the largest layer thickness, applications that require thin layers may suffer from a drop in mechanical properties if going bio-based.

Synthetic methacrylate and acrylate resins are transparent and present few or no printing defects. Vanillin and vegetable oil resins are colorless or slightly yellow while resins containing lignin have a deeper brown color. Overall, the quality of the prints is of a high standard with good adhesion between the layers and the possibility to print rigid, complex shapes. Similarly to the epoxy resins, some components of the material, such as lignin and eugenol, give a brown color and can hinder the transparency of the material (Fig. 7). The Young's moduli of the some of the acrylate and methacrylate resins reviewed in this work exceed the epoxy ones, ranging from 7.89 MPa to 4903 MPa, vegetable oil methacrylate and acrylate resins exhibits weaker young's moduli, while vanillin produce stiffer and stronger material (Table 3).

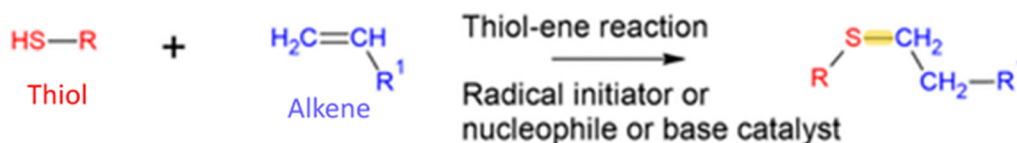
### 3.3. Thiol-ene resins

Thiol-ene resins rely on the use of the reaction between a thiol and an alkene to form a thioether called thiol-ene click reaction (Fig. 8).

Resins based on a thiol-ene click reaction have demonstrated a potential for AM because they have low shrinkage stress and the thiol-ene reactions are fast and generate a high yield.<sup>57,58</sup> They also have the potential to make tough and flexible materials.<sup>58</sup> The results obtained in the works reviewed show that thiol-ene resins have not yet reached their potential in additive manufacturing in terms of mechanical properties. They generally exhibit a lower stiffness than acrylates and epoxies, with Young's moduli ranging from 0.4 to around 900 MPa (Table 3). These resins are interesting because the thiol-ene reactions are fast and generate a high yield.

Other thiol-ene bio-based reactions without levoglucosan are also being developed for additive manufacturing such as the limonene and  $\beta$ -myrcene reaction.<sup>59</sup>

Levoglucosenone and levoglucosan thiol-ene prints made by vat photopolymerization show defects, they have irregular shapes (Fig. 9a and b) and heterogeneous color (Fig. 9a), this is not the case for the LDM printed levoglucosan resin which achieves good print fidelity.<sup>19</sup> In the case of thiol-ene polymers, LDM additive manufacturing allows for better print quality, however, thiol-ene resins are photocured which means a UV



R and R1 represent generic monomeric or oligomeric groups

Fig. 8 Schematic representation of the thiol-alkene reaction.



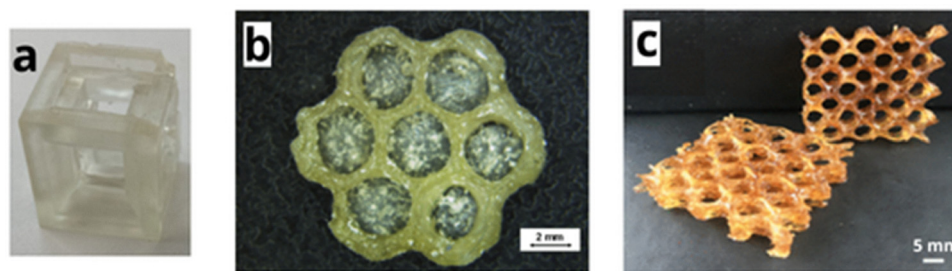


Fig. 9 (a) Levoglucosan thiol-ene resin print Reproduced with permission from American Chemical Society, copyright 2024<sup>61</sup> (b) Levoglucosan thiol-ene resin print<sup>57</sup> (c) Limonene thiol-ene resin print Reproduced with permission from American Chemical Society, copyright 2022.<sup>59</sup>

lamp is needed to flash the print for 10 seconds between each layer making this technique highly time consuming compared to vat photopolymerization. The thiol-ene resins are translucent for the most part but not as transparent as some of the methacrylate and acrylate resins (Fig. 7b). The shape memory response that thiol-ene polymers exhibit makes them suitable for biomedical applications.<sup>58–60</sup>

### 3.4. Other bio-based resins

Other types of thermosetting resins have also been explored for additive manufacturing, *i.e.*: (i) resins with ester linkages have been developed, but even if they integrate bio-based compounds they also rely on petroleum based precursors;<sup>62,63</sup> (ii) ester linkages have also been coupled with methacrylate and thiol-ene chemistry<sup>56,64</sup> and (iii) bio-based polyesters have been formulated from various sources: such as sebacic acid, succinic acid, isophthalic acid, phthalic anhydride, 2,5 furandicarboxylic acid, citric acid and terpenes derivatives. Compared to other reviewed bio-based resins they can be nontoxic, however, their tensile strength of 4–5 MPa and Young's modulus of less than 100 MPa, pale in comparison with commercial resins, other reported polyesters have shown better mechanical properties but they have been applied to additive manufacturing yet.<sup>64</sup> Poly(furfuryl alcohol) usage has been reported in combination with carbon nanotubes in order to obtain electrically conductive thermoset composites.<sup>65</sup> Additionally, poly(octanediol citrate), a bio-based elastomer, has been successfully printed, this polymer is an elastomer derived from citric acid and has the advantage of being nontoxic, the curing kinetics of this elastomer are the longest of any reported in this reviewed with 3 days at 80 °C in vacuum making the process inefficient.<sup>66</sup>

While the topic of bio-based thermoset additive manufacturing is growing, it is surprising that common bio-based thermosets have not been reported for their use in additive manufacturing yet, phenolic resins for example are extensively investigated but the main focus for these polymers remains wood based panels.<sup>67</sup> Even more surprising thermosetting polyurethanes have not been reported in additive manufacturing despite having been identified as a way to enhance toughness for bio-based acrylic resins.<sup>68</sup>

Overall, the thickness of printed layers is determined more by the additive manufacturing technique than by the type of resin used. Layer size for both bio-based and commercially available resins typically range from 20  $\mu\text{m}$  and 100  $\mu\text{m}$  in vat

photopolymerization and from 200  $\mu\text{m}$  to 1300  $\mu\text{m}$  in extrusion-based printing.<sup>22,34</sup> UV-based additive manufacturing techniques generally produce thinner layers than the extrusion-based methods, making them more suitable for biomedical applications. However, the mechanical and rheological properties of printed materials are significantly impacted by the type of resin. Acrylate, methacrylate and epoxy resins tend to exhibit higher storage moduli and greater toughness than thiol-ene resins. While not reported in Table 3 it is noteworthy that strain at break, which is usually low for thermosets (< 5%) tend to be higher for bio-based thermosets than synthetic ones, the reason for this is the lower crosslinking density for bio-based thermosets.<sup>44</sup> Vat photopolymerization is also more common than extrusion-based techniques for the additive manufacturing of bio-based thermosets (Table 3).

## 4. Bio-based fillers for the AM of thermosetting bio composites

A bio composite is constituted of a polymer matrix and bio-based filler, these fillers are fibers or particles harvested from biomass. The original goal behind the use of bio-based fibers in combination with petroleum-based polymers was to increase the sustainability of existing materials.<sup>73</sup> It is possible to increase recyclability by using natural fibers that will be separated more easily from the matrix, because natural fibers decompose or burn more easily compared to synthetic ones. Although the thermoset matrix recycling is still challenging.<sup>74</sup> In additive manufacturing, bio-based fillers have been used with thermosets such as urea formaldehyde<sup>75,76</sup> or petroleum-based epoxy.<sup>77</sup> Bio-based fillers can also be used in combination with a bio-based matrix to create a 100% bio-based composite.

Beyond their sustainability benefits, bio-based fillers can improve the mechanical properties and dimensional stability of materials.<sup>78,79</sup> The compatibility between matrix and filler is often the main drawback for bio-based fillers<sup>74</sup> which can lead to lower dimensional stability and poor mechanical properties but this challenge is well understood and filler treatments improving adhesion have been reported.<sup>66,71</sup> Furthermore, when sourced as by-products from other industries such as wood powder, lignin or other bio-wastes, they help reduce overall material costs.



Table 3 Overview of research works on the additive manufacturing of bio-based thermosetting polymers

AM technology	Bio-based feedstock	Primary functional group	Curing conditions	Rheological behavior	Layer thickness	Mechanical properties of the material	Additional characteristics	Source
LDM	Levogluconan from cellulosic biomass	Thiol and alkene	UV light: intensity 25 mW cm <sup>-2</sup> for 10s per layer + 100 mW cm <sup>-2</sup> for 15 min at the end 200 °C for 6 h	Storage modulus at 25 °C: around 50 MPa Viscosity: around 500 Pa s Storage modulus 25 °C: around 2500 MPa Loss modulus 25 °C: around 800 MPa Viscosity: 2000–40000 Pa s	200 μm	Young's modulus: 14.49 ± 0.58 MPa Tensile strength: 2.73 ± 0.67 MPa	Hydrolytic degradation possible	19
	Cardanol	Epoxy	—	Storage modulus at 25 °C: around 1 MPa Loss modulus at 25 °C: around 0.4 MPa Viscosity 25 °C: around 1000 Pa s	400 μm	—	Vitrimer Recyclable	18
	Commercial poly(furfuryl alcohol)	Furfuryl alcohol	—	Storage modulus at 25 °C: around 1 kPa Loss modulus at 25 °C: around 0.3 kPa Viscosity 25 °C: around 10000 Pa s	450 μm	—	Electrically conductive Use of direct ink write (DIW)	65
	Citric acid	Poly(1, 8-octanediol-co-Pluronic F127 citrate)	80 °C for 3 days (in vacuum)	Storage modulus at 25 °C: around 1 kPa Loss modulus at 25 °C: around 0.3 kPa Viscosity 25 °C: around 10000 Pa s	500–600 μm	Compression modulus: around 5 MPa	Elastomer Use of Direct ink write (DIW)	66
	Coconut oil, glycerol, sebacic acid and citric acid	Ester	105 °C for 48 h	—	1200 μm	Compressive strength as maximum stress in plateau region: ≈ 0.7 MPa Young modulus: 1025 ± 130 MPa Fracture energy: 245 ± 35 Pa	—	63
	Commercial bio-epoxy	Epoxy	25 °C for 6 h	Viscosity 25 °C: 1.6–110 Pa s increasing with filler content	1300 μm	Young modulus: 1025 ± 130 MPa Fracture energy: 245 ± 35 Pa	Delayed extrusion of cold masterbatch (DECMA), technique slightly different than LDM	20
SLA	Lignin	Acrylate and methacrylate	UV/Visible 405 nm Post curing: UV light for 3 min	Viscosity 25 °C: around 700 mPa s	26–50 μm	Young's modulus: 480 ± 10 MPa Tensile strength: 18 ± 1 MPa	Composite with 10% wt lignin	44
	Limonene	Thiol and alkene	UV 365 nm Post curing: UV 365 nm	Storage modulus UV: 11 MPa Loss modulus UV: 0.167 MPa	50 μm	Young's modulus: 43.8 MPa Tensile strength: 24.4 MPa Toughness: 2740 Pa	—	69
	Linalool	Thiol and alkene	UV 365 nm 120 °C for 12 h	Storage modulus UV: 12 MPa Loss modulus UV: 0.149 MPa Storage modulus UV: 13200 MPa Loss modulus UV: 0.015 MPa	50 μm	Young's modulus: 0.4 MPa Tensile strength: 2.8 MPa Toughness: 149 Pa	—	69
	Nerol	Thiol and alkene	UV 365 nm Post curing: 120 °C for 12 h	Storage modulus UV: 6700 MPa Loss modulus UV: 0.107 MPa	50 μm	Young's modulus: 0.5 MPa Tensile strength: 2.4 MPa Toughness: 103 Pa	—	69
	Geraniol	Thiol and alkene	UV 365 nm Post curing: 120 °C for 12 h	Storage modulus UV: 6700 MPa Loss modulus UV: 0.107 MPa	50 μm	Young's modulus: 0.4 MPa Tensile strength: 2.4 MPa Toughness: 129 Pa	—	69



Table 3 (continued)

AM technology	Bio-based feedstock	Primary functional group	Curing conditions	Rheological behavior	Layer thickness	Mechanical properties of the material	Additional characteristics	Source
	Vanillyl alcohol, eugenol and Guaiacol	Acrylate, methacrylate and thiol-ene	UV 365 nm: intensity $2.6 \pm 0.4 \text{ mW cm}^{-2}$ Post curing: 120 °C for 12 h	Storage modulus at 25 °C: 3400 MPa Loss modulus at 25 °C: around 1000 MPa	60–90 $\mu\text{m}$ (set to 100 $\mu\text{m}$ )	Young's modulus: $1230 \pm 70 \text{ MPa}$ Tensile strength: $61.7 \pm 5.1 \text{ MPa}$ Toughness: $3.7 \pm 0.9 \text{ MPa}$	—	46
	Soybean oil (75%)	Thiol and alkene (75%)	UV light: intensity 9.3 W $\text{cm}^{-2}$	Storage modulus UV: $3.96 \pm 0.00 \text{ MPa}$ Loss modulus UV: $12.56 \pm 0.00 \text{ kPa}$ Complex viscosity UV: $63.03 \pm 0.00 \text{ MPa s}$ Viscosity 25 °C: $4030 \pm 20 \text{ mPa s}$	80–100 $\mu\text{m}$	Young's modulus: $8.76 \pm 2.22 \text{ MPa}$	Mix of two resins	26
	Linseed oil (25%)	Thiol and epoxy (25%)	Post curing: 150 °C for 1 h	Storage modulus UV: $4030 \pm 20 \text{ mPa s}$ Loss modulus UV: around 1.5 GPa Viscosity: <20 Pa s	100 $\mu\text{m}$	Tensile strength: $0.87 \pm 0.01 \text{ MPa}$	—	34
	Furan dimethanol from vegetable biomass carbohydrates	Epoxy	UV 375 nm: intensity $70 \text{ W cm}^{-2}$ and 80 °C	Storage modulus UV: around 1.5 GPa Viscosity: <20 Pa s	100 $\mu\text{m}$	Young's modulus: $1924 \pm 86 \text{ MPa}$ Tensile strength: $45 \pm 9 \text{ MPa}$ Toughness: $1.23 \pm 0.23 \text{ MPa}$	—	34
	Resorcinol	Epoxy	UV 375 nm: intensity $70 \text{ W cm}^{-2}$ and 80 °C	Storage modulus UV: around 1.5 GPa Viscosity: <20 Pa s	100 $\mu\text{m}$	Young's modulus: $2355 \pm 45 \text{ MPa}$ Tensile strength: $79 \pm 11 \text{ MPa}$ Toughness: $2.03 \pm 0.27 \text{ MPa}$	—	28
	Soybean oil	Epoxy	UV 375 nm: intensity $70 \text{ W cm}^{-2}$ and 100 °C	Storage modulus UV: around 200 MPa Loss modulus UV: around 200 MPa Viscosity 25 °C: 400–600 mPa s	100 $\mu\text{m}$	Young's modulus: $0.37 \pm 0.10 \text{ MPa}$ Tensile strength: $2.1 \pm 0.8 \text{ MPa}$ Toughness: $100 \pm 21 \text{ Pa}$	Possible degradation in alkali	28
	Linseed oil	Epoxy	UV 375 nm: intensity $70 \text{ W cm}^{-2}$ and 100 °C	Storage modulus UV: around 200 MPa Loss modulus UV: around 200 MPa Viscosity 25 °C: 800–1300 mPa s	100 $\mu\text{m}$	Young's modulus: $5.1 \pm 0.2 \text{ MPa}$ Tensile strength: $16.2 \pm 1.0 \text{ MPa}$ Toughness: $1990 \pm 370 \text{ Pa}$	Possible degradation in alkali	28
	Vanillin	Acrylate and methacrylate	UV light program	Storage modulus at 25 °C: $2500 \pm 300 \text{ MPa}$ Loss modulus at 25 °C: around 150 MPa Viscosity 25 °C: $99 \pm 1 \text{ mPa s}$	100 $\mu\text{m}$	Young's modulus: $2920 \pm 149 \text{ MPa}$ Tensile strength: $20.27 \pm 2.24 \text{ MPa}$	—	47
	Vanillin	Acrylate and methacrylate	UV light program Post curing: UV/visible 405 nm at 80 °C for 2 h	Storage modulus at 25 °C: $3800 \pm 300 \text{ MPa}$ Loss modulus at 25 °C: around 10 MPa Viscosity 25 °C: $99 \pm 1 \text{ mPa s}$	100 $\mu\text{m}$	Young's modulus: $4903 \pm 120 \text{ MPa}$ Tensile strength: $12.49 \pm 1.63 \text{ MPa}$	—	47



Table 3 (continued)

AM technology	Bio-based feedstock	Primary functional group	Curing conditions	Rheological behavior	Layer thickness	Mechanical properties of the material	Additional characteristics	Source
	Levoglucozan from cellulosic biomass	Thiol and alkene	UV 320 nm Post curing: UV light for 1 min	—	—	Tensile strength: 3.41 MPa Young's modulus: around 4 MPa	—	61
	2,5-Furandicarboxylic acid	Ester	UV/Visible 405 nm: intensity 40 mW cm <sup>-2</sup> Post curing: light for 30 min	Storage modulus UV: around 1 MPa Viscosity 20 °C: 4690 mPa s	20 μm	—	—	62
	Succinic acid	Ester	UV/Visible 405 nm: intensity 40 mW cm <sup>-2</sup> Post curing: light for 30 min	Storage modulus UV: around 4 MPa Viscosity 20 °C: 1210 mPa s	20 μm	—	—	62
	Sebacic acid	Ester	UV/Visible 405 nm: intensity 40 mW cm <sup>-2</sup> Post curing: light for 30 min	Storage modulus UV: around 1 MPa Viscosity 20 °C: 740 mPa s	20 μm	—	—	62
DLP	Isophthalic acid	Ester	UV/Visible 405 nm: intensity 40 mW cm <sup>-2</sup> Post curing: light for 30 min	Storage modulus UV: around 1 MPa Viscosity 20 °C: 3030 mPa s	20 μm	—	—	62
	Phthalic anhydride	Ester	UV/Visible 405 nm: intensity 40 mW cm <sup>-2</sup> Post curing: light for 30 min	Storage modulus UV: around 1 MPa Viscosity 20 °C: 5140 mPa s	20 μm	—	—	62
	Linseed oil and eugenol	Acrylate	UV/Visible 405 nm Post curing: Thermal 180 °C for 30 min	Storage modulus at 25 °C: 884 MPa Viscosity 30 °C: <900 mPa s	25 μm	—	Shape memory	52
	Cellulose-derived levoglucosenone	Thiol and alkene	UV 385 nm: intensity 100 mW cm <sup>-3</sup> for 1 min Post curing: UV for 1 min	Storage modulus UV 80 °C: around 100 kPa Viscosity 80 °C: 20 000 mPa s	50 μm	Young's modulus: 4.2 ± 0.7 MPa Tensile strength: 3.1 ± 0.5 MPa	—	70
	Vanillin and eugenol	Methacrylate	UV light	—	—	Young's modulus: 12 MPa Tensile strength: 0.4 MPa	—	71
	Vanillin	Methacrylate	UV 385 nm: intensity 28.8 mW cm <sup>-2</sup> Post curing: UV/visible 385 nm for 6 min + thermal 30 °C until constant weight	Storage modulus UV: 217 ± 21 kPa	50 μm	Young's modulus: 1020 ± 140 MPa Tensile strength: 51.2 ± 10.2 MPa	Vitrimer-like behavior The carbon-dot filler decreases mechanical properties	49
	Levoglucozan from cellulosic biomass	Thiol and alkene	UV 365 nm: intensity 25 mW cm <sup>-2</sup>	Storage modulus UV: around 500 Pa Viscosity 25 °C: around 20 000 mPa s	100 μm	Young's modulus: 12.3 ± 1.0 MPa Tensile strength: 8.2 ± 0.6 MPa Toughness: 6.33 ± 0.61 MPa	Possible degradation in alkali	57
	Glycerol (40%)	Acrylate (40%)	UV 385 nm, intensity 9.8 mW cm <sup>-2</sup>	Storage modulus UV: 224.5 ± 5.8 MPa Loss modulus UV: 134.5 ± 1.6 MPa Complex viscosity UV: 8.4 ± 0.5 GPa s	100 μm	—	Mix of two resins shape memory Reparable	50



Table 3 (continued)

AM technology	Bio-based feedstock	Primary functional group	Curing conditions	Rheological behavior	Layer thickness	Mechanical properties of the material	Additional characteristics	Source
	Tetrahydrofurfuryl methacrylate (60%) Soybean oil	Methacrylate (60%) Methacrylate	UV/visible 390–450 nm Post curing: UV/visible 405 nm 39 W at 60 °C for 30 min UV 385 nm: intensity 28 mW cm <sup>-2</sup> Post curing: UV for 2 min UV/Visible 405 nm	Viscosity 25 °C: 1394 mPa s Storage modulus at 30 °C: around 40 MPa Viscosity: around 0.8 Pa s	100 μm	Young's modulus: 1007 ± 30 MPa Tensile strength: 43.7 ± 0.3 MPa	—	51
	Lactic acid	Ester and methacrylate	UV 385 nm: intensity 28 mW cm <sup>-2</sup> Post curing: UV for 2 min UV/Visible 405 nm	Storage modulus 25 °C: 1780 MPa Viscosity at 25 °C: 451 ± 16 mPa s	100 μm	Young's modulus: 3700 ± 200 MPa Tensile strength: 89 ± 5 MPa	Possible upcycling by aminolysis	56
	Limonene	Epoxy and methacrylate	Post curing: UV/Visible 405 nm 1 h/40 °C + thermal 30 min at 150 °C UV/Visible	—	—	—	—	55
	Tartaric acid from grapes	Methacrylate	UV/Visible Post curing: UV/Visible 100 mW cm <sup>-2</sup> for 10 min	Storage modulus at 25 °C: 3.9 GPa Viscosity: 13 750 mPa s	100–500 μm	Young's modulus: 1244.2 MPa Tensile strength: 104.4 MPa Toughness: 6.3 MPa Young's modulus: 322.2 MPa Tensile strength: 2.0 MPa	Vitriimer Self-healing	72
	Vanillin	Acrylate	UV/Visible light	—	—	—	Vitriimer	48
	Eugenol	Acrylate	Post curing: UV/Visible 405 nm for 24 h UV/Visible light	—	—	Young's modulus: 419.7 MPa Tensile strength: 5.0 MPa	Vitriimer	48
	Guaiacol	Acrylate	Post curing: UV/Visible 405 nm for 24 h UV/Visible light	—	—	Young's modulus: 301.8 MPa Tensile strength: 2.2 MPa	Vitriimer	48
	Limonene	Thiol and alkene	Post curing: UV/Visible 405 nm for 24 h UV/Visible 405 nm	Storage modulus 25 °C: around 1000 MPa Loss modulus 25 °C: around 140 MPa Viscosity 25 °C: 60 000 mPa s	—	Young's modulus: around 900 MPa Tensile strength: around 55 MPa	Shape memory Cytocompatible	59
	β-Myrcene	Thiol and alkene	UV/Visible 405 nm	Storage modulus 25 °C: around 8 MPa Loss modulus 25 °C: around 10 MPa	—	Tensile strength: around 2.5 MPa	Shape memory Cytocompatible	59
LCD	Vanillin soybean oil and lignin	Acrylate and methacrylate	UV/Visible 405 nm Post curing: UV/Visible 405 nm for 24 h	—	—	Young's modulus: 7.89 ± 0.82 MPa	Self-healing	45
	Palm oil and eugenol	Methacrylate and acrylamide	UV/visible 405 nm: intensity 300 mW cm <sup>-2</sup> Post curing: UV/visible 405 nm 300 mW cm <sup>-2</sup> for 6 min	Storage modulus 25 °C: around 1800 MPa Viscosity 25 °C: 1400 mPa s	50 μm	Tensile strength: around 15 MPa Flexural strength: around 60 MPa	Can be degraded and reprinted	53



Table 3 (continued)

AM technology	Bio-based feedstock	Primary functional group	Curing conditions	Rheological behavior	Layer thickness	Mechanical properties of the material	Additional characteristics	Source
	Palm oil	Methacrylate and acrylate	UV/Visible 405 nm Post curing: UV 365 nm 40 mW cm <sup>-2</sup> for 5 min	Storage modulus 25 °C: around 1500 MPa Viscosity 25 °C: 50 mPa s	50 μm	Tensile strength: around 50 MPa Flexural strength: around 55 MPa	Shape memory	54
	Limonene, geraniol and linalool	Ester and thioether	UV/visible 405 nm Post curing: UV/visible 34.7 mW cm <sup>-2</sup> for 20 min	Storage modulus 25 °C: around 1000 MPa Viscosity 25 °C: 8900 ± 800 mPa s	100 μm	Young's modulus: <100 MPa Tensile strength: 4–5 MPa	—	64

In extrusion-based additive manufacturing processes, the nozzle can be clogged due to the use of fillers which is a major challenge when incorporating fillers.<sup>80</sup> Clogging occurs when the particle/nozzle ratio is too great, it is possible to decrease clogging by increasing the nozzle diameter or decreasing particle size.<sup>81</sup> Reducing fillers size requires additional processing while increasing nozzle size will also increase layer size and be less precise. Additionally, the difficult separation of thermosetting polymers and bio-based fillers is a downside for recyclability, even if ongoing research aims to develop improved recycling methods for these materials.<sup>82</sup>

#### 4.1. Micro scale bio-based fillers

Wood in fine particle form is frequently present as reinforcements in thermoplastic<sup>83</sup> and thermosetting composites.<sup>20,75,76</sup> Wood particles are one of the main by-product of the various wood-processing industries.<sup>84</sup> The use of wood flour in combination with urea formaldehyde polymers is frequent because it draws inspiration from a different field than additive manufacturing: the wood panel industry, where urea formaldehyde is usually used to bond wood to make wood-based panels.<sup>75,76</sup> The presence of wood particles in composites can increase the tensile strength by 617% when adding up to 10% wt wood flour to a methacrylate matrix.<sup>71,85</sup> In this case, the wood particle was previously methacrylated to enhance its affinity with the polymer matrix. The modified wood flour is functionalized and participates to the cross-linking warping the actual effect of the filler.<sup>71</sup> The second biggest improvement in tensile strength is lower with a 281% increase with 5% wt micro-scale bamboo fibers, it is not surprising because fibers usually provide a higher increase in tensile strength compared to particles because of their higher aspect ratios.<sup>86</sup>

#### 4.2. Nano scale bio-based fillers

Composites with nanofillers, often referred to as nanocomposites, have the potential to broaden the range of materials that can be developed for additive manufacturing by adding functionalities and increasing mechanical properties. Furthermore, the size of nanofillers is advantageous because it reduces the risk of nozzle clogging in extrusion based additive manufacturing techniques. Cellulose nano crystals<sup>77,87</sup> have been, for instance, incorporated into an epoxy matrix to increase mechanical strength with 1% wt and 2% wt cellulose nano crystals tensile strength increased by 12 and 19% respectively.<sup>87,88</sup> With 5% wt the opposite effect is reported with a decrease of tensile strength by 6%. This is potentially due to the agglomeration of fillers.<sup>89</sup> The same observation has also been reported with lower cellulose nano crystals content in a methacrylate matrix, with an increase of 30% in tensile strength with 0.5% wt of cellulose nano crystals, while with a 1% wt load of filler the tensile strength drops back down to equal the neat resin. Chitin nanocrystals were also used as nanofillers in additive manufacturing,<sup>66</sup> they provided a 99% increase in stress at 40% strain in wet state and a 96% in dry state, this massive jump in initial modulus is made possible thanks to the strong interactions between the polymer and the matrix which



created extra crosslinks and is specifically tailored to the use with poly(1, 8-octanediol-*co*-Pluronic F127 citrate).<sup>66,90</sup> Bio-based nano fillers are not limited to increasing existing materials properties but can also create new functionalities altogether, bio-based carbon dots, derived from  $\alpha$ -cellulose, are used to create electrically conductive materials.<sup>49</sup> These carbon dots are also a rare occurrence of fillers decreasing the mechanical properties of the material with a 56% decrease of stress at break with 1% wt carbon dots, this is due to the light absorption of carbon dots which reduces the matrix ability to cure, creating less covalent crosslinks (Table 4).<sup>49</sup>

Bio-based fillers offer an increase in tensile strength and rigidity of the material but there are some exceptions: if the filler load is too important it can cause agglomeration which decreases tensile strength,<sup>87,89</sup> bubbles can be created in the polymer matrix which make the mechanical strength plummet,<sup>20</sup> finally in VAT photopolymerization if the filler absorbs light it can hinder crosslinking decreasing mechanical properties.<sup>49</sup> Bio-based fillers also increase the viscosity of the resin in all formulations, it can be an advantage to allow the shape to be maintained after printing and before complete curing in

**Table 4** Overview of research works on the additive manufacturing thermosets with bio-based fillers

AM technology	Bio-based filler	Particle size	Polymer matrix	Curing conditions	Changes of mechanical properties with addition of filler	Sources	
LDM	Cellulose nano crystals	Nano scale	Branched polyester	105 °C for 48 h	No comparison with pure resin	65	
	Chitin nano crystals	Nano scale	Poly(1, 8-octanediol- <i>co</i> -Pluronic F127 citrate) (Elastomer)	80 °C for 3 days (in vacuum)	With 40% wt: increase stress at 40% strain dry by 96%	66	
	Cellulose powder and carbon nanotubes	50% of cellulose particles < 9.8 $\mu$ m	Poly(furfuryl alcohol)	—	—	65	
	Cellulose powder	< 12 $\mu$ m	Bio-epoxy resin	200 °C for 6 h	—	9	
	Wood particles	< 75 $\mu$ m	Urea formaldehyde	Thermal curing cycle Printing bed: 60 °C + 3 °C every layer Thermal post curing: 100 °C for 1 h	No comparison with pure resin	75	
	Bio char from spent coffee ground	20–75 $\mu$ m	Epoxy resin		25 °C for 6 h	With 1% wt filler: 43.3% increase in flexural strength	91
	Lignin	64 $\pm$ 35 $\mu$ m	Bio-epoxy resin	25 °C for 6 h	Decrease in tensile strength	20	
	Sawdust	189 $\pm$ 104 $\mu$ m	Bio-epoxy resin	25 °C for 6 h	Decrease in tensile strength	20	
Wood particles	< 237 $\mu$ m	Urea formaldehyde	Printing bed: 80 °C Thermal post curing: 50 °C for 2 h + 7 days room temperature	No comparison with pure resin	76		
SLA	Cellulose nano crystals	Diameter 3 $\pm$ 1 nm Length 246 $\pm$ 100 nm	Methacrylate elastomer	UV/Visible light	With 0.5% wt filler: 30% Increase in tensile strength	87	
	Cellulose nano crystals	Diameter 15 $\pm$ 5 nm Length 220 $\pm$ 61 nm	Epoxy resin	Post curing: UV/Visible light at 60 °C for 1 h UV light	With 1% wt filler: No change in tensile strength With 1 and 2% wt: 12 and 19% increase in tensile strength respectively	77	
	Walnut shell powder	< 45 $\mu$ m	Bio-epoxy resin	UV at 100 °C	With 5% wt: 6% decrease in tensile strength With 10 and 20% wt: up to 469 and 743% increase in tensile toughness respectively	28	
	Walnut shell powder	< 75 $\mu$ m	Bio-epoxy resin	UV at 100 °C	With 10 and 20% wt: up to 326 and 469% increase in tensile toughness respectively	28	
	Hemp powder	< 75 $\mu$ m	Bio-epoxy resin	UV at 100 °C	With 10 and 20% wt: up to 380 and 371% increase in tensile toughness respectively	28	
	Tagua nut powder	< 75 $\mu$ m	Bio-epoxy resin	UV at 100 °C	With 10 and 20% wt: up to 186 and 254% increase in tensile toughness respectively	28	
DLP	Carbon dots from $\alpha$ -cellulose	Nano scale	Vanillin methacrylate resin	UV light: intensity 28.8 mW cm <sup>-2</sup> Post curing: UV for 6 min + thermal 30 °C until constant weight	UV light	With 1% wt filler: 56% decrease of tensile stress at break	49
	Methacrylated wood flour	2–30 $\mu$ m	Eugenol and vanillin methacrylate	UV light	With 10% wt filler: 617% increase in tensile strength	71	
LCD	Micro-scale bamboo fibers	Width 21.1 $\mu$ m Length 192 $\mu$ m	Palm oil fatty acid-ethyl acrylamide and methacrylated eugenol	UV/visible light: intensity 300 mW cm <sup>-2</sup> Post curing: UV/visible 300 mW cm <sup>-2</sup> for 6 min	With 1,3 and 5% wt filler: 90%, 257% and 281% increase in tensile strength respectively	53	



extrusion-based AM.<sup>92,93</sup> For both VAT photopolymerization and extrusion-based AM viscosity should be maintained to a low enough level where it will not hinder processability, which can make the choice of the concentration of filler challenging.<sup>89</sup>

VAT photopolymerization was prevalent in the additive manufacturing of bio-based thermosetting resins, however, when fillers are present in the formulation, extrusion-based processes seem to be more common (Table 4). The reason for this could be that light curing can be obstructed by the filler making it more difficult for UV light reliant techniques and making the extrusion-based methods more suitable.

## 5. Conclusion

This review shows the potential of bio-based constituents in the additive manufacturing of thermosets and how their implementation could change this field traditionally dominated by petroleum-based materials. Epoxy and methacrylate resins can incorporate bio-based constituents while preserving printability and mechanical properties similar to commercial petroleum-based resins. Other resin types also exhibit promising properties for different applications, in particular, thiol-ene resins which offer excellent shape memory response making them suitable for biomedical applications. This review also explored the use of bio-based fillers and their role in the additive manufacturing of thermosets, not only by increasing sustainability but also by allowing the valorization of under-used by-products or enhancing the mechanical properties of printed materials. The different additive manufacturing techniques that allow these novel materials to be processed are also reviewed showing the duality between vat photopolymerization, which allows for better print quality and is more widely used and extrusion-based techniques, more suitable for thermosetting bio composites additive manufacturing. Further technological developments in this domain are to be expected, especially to solve challenges such as the reliance on petroleum based photoinitiator, and the understanding of the curing kinetics of bio-based thermosets. The increasing demand for multifunctional bio-based materials, together with the encouraging outcomes of ongoing research, is anticipated to drive the development of industrially scalable materials and more sustainable manufacturing processes, thereby generating positive economic, societal, and environmental impacts.

## Conflicts of interest

The authors declare that they have no competing interests.

## Data availability

No primary research results, software or code have been included and no new data were generated or analysed as part of this review.

## Acknowledgements

This work was supported by Association Nationale Recherche Technologie (ANRT) under grant agreement no. 2024/0076 and by the ROBUSTOO Project funded by the European Union under grant agreement no. 101135119.

## References

- 1 M. B. A. Tamez and I. Taha, A review of additive manufacturing technologies and markets for thermosetting resins and their potential for carbon fiber integration, *Addit. Manuf.*, 2021, **37**, 101748, DOI: [10.1016/j.addma.2020.101748](https://doi.org/10.1016/j.addma.2020.101748).
- 2 Q. Guo, *Thermosets: Structure, properties and applications*, Woodhead Publishing in Materials, 2017.
- 3 A. Dodiuk and S. H. Goodman, *Handbook of Thermoset Plastics*, Plastics-William Andrew, 2014.
- 4 B. Wang, Z. Zhang, Z. Pei, J. Qiu and S. Wang, Current progress on the 3D printing of thermosets, *Adv. Compos. Hybrid Mater.*, 2020, **3**(4), 462–472, DOI: [10.1007/s42114-020-00183-z](https://doi.org/10.1007/s42114-020-00183-z).
- 5 R. Mahshid, M. N. Isfahani, M. Heidari-Rarani and M. Mirkhalaf, Recent advances in development of additively manufactured thermosets and fiber reinforced thermosetting composites: Technologies, materials, and mechanical properties, *Composites, Part A*, 2023, **171**, 107584, DOI: [10.1016/j.compositesa.2023.107584](https://doi.org/10.1016/j.compositesa.2023.107584).
- 6 J. Su, W. L. Ng, J. An, W. Y. Yeong, C. K. Chua and S. L. Sing, Achieving sustainability by additive manufacturing: a state-of-the-art review and perspectives, *Virtual Phys. Prototyping*, 2024, **19**(1), e2438899, DOI: [10.1080/17452759.2024.2438899](https://doi.org/10.1080/17452759.2024.2438899).
- 7 F. Zhang, *et al.*, The recent development of vat photopolymerization: A review, *Addit. Manuf.*, 2021, **48**, 102423, DOI: [10.1016/j.addma.2021.102423](https://doi.org/10.1016/j.addma.2021.102423).
- 8 A. Bagheri and J. Jin, 'Photopolymerization in 3D Printing', *ACS Appl. Polym. Mater.*, 2019, **1**(4), 593–611, DOI: [10.1021/acsapm.8b00165](https://doi.org/10.1021/acsapm.8b00165).
- 9 B. Redwood, F. Schöffner and B. Garret, *The 3D Printing Handbook\_ Technologies, design and applications*, 3D Hubs, 2017.
- 10 C. W. Hull and S. Gabriel, Apparatus For Production Of Three-Dimensional Objects By Stereo Thography.
- 11 H. Quan, T. Zhang, H. Xu, S. Luo, J. Nie and X. Zhu, Photocuring 3D printing technique and its challenges, *Bioact. Mater.*, 2020, **5**(1), 110–115, DOI: [10.1016/j.bioactmat.2019.12.003](https://doi.org/10.1016/j.bioactmat.2019.12.003).
- 12 M. Pagac, *et al.*, A Review of Vat Photopolymerization Technology: Materials, Applications, Challenges, and Future Trends of 3D Printing, *Polymers*, 2021, **13**(4), 598, DOI: [10.3390/polym13040598](https://doi.org/10.3390/polym13040598).
- 13 H.-W. Chen, J.-H. Lee, B.-Y. Lin, S. Chen and S.-T. Wu, Liquid crystal display and organic light-emitting diode display: present status and future perspectives, *Light: Sci. Appl.*, 2017, **7**(3), 17168, DOI: [10.1038/lsa.2017.168](https://doi.org/10.1038/lsa.2017.168).



- 14 Z. Zhu, Freeform Optics for Achieving Collimated and Uniform Light Distribution in LCD-Type UV-Curable 3D Printing, *IEEE Photonics J.*, 2023, **15**(4), 1–7, DOI: [10.1109/JPHOT.2023.3294478](https://doi.org/10.1109/JPHOT.2023.3294478).
- 15 I. A. Tsolakis, W. Papaioannou, E. Papadopoulou, M. Dalampira and A. I. Tsolakis, 'Comparison in Terms of Accuracy between DLP and LCD Printing Technology for Dental Model Printing', *Dentistry J.*, 2022, **10**(10), 181, DOI: [10.3390/dj10100181](https://doi.org/10.3390/dj10100181).
- 16 Springer Handbook of Additive Manufacturing, ed. E. Pei, *et al.*, in *Springer Handbooks*, Springer International Publishing, Cham, 2023, DOI: [10.1007/978-3-031-20752-5](https://doi.org/10.1007/978-3-031-20752-5).
- 17 K. Bouzidi, Formulation of a thermosetting biocomposite based on poly (furfuryl alcohol) and cellulose for 3D printing, 2023.
- 18 J. M. Capannelli, S. Dalle Vacche, A. Vitale, K. Bouzidi, D. Beneventi and R. Bongiovanni, 'A biobased epoxy vitrimer/cellulose composite for 3D printing by Liquid Deposition Modelling', *Polym. Test.*, 2023, **127**, 108172, DOI: [10.1016/j.polymertesting.2023.108172](https://doi.org/10.1016/j.polymertesting.2023.108172).
- 19 M. K. Porwal, M. M. Hausladen, C. J. Ellison and T. M. Reineke, 'Biobased and degradable thiol-ene networks from levoglucosan for sustainable 3D printing', *Green Chem.*, 2023, **25**(4), 1488–1502, DOI: [10.1039/D2GC04185E](https://doi.org/10.1039/D2GC04185E).
- 20 J. Trifol, *et al.*, 3D-Printed Thermoset Biocomposites Based on Forest Residues by Delayed Extrusion of Cold Masterbatch (DECMA), *ACS Sustainable Chem. Eng.*, 2021, **9**(41), 13979–13987, DOI: [10.1021/acssuschemeng.1c05587](https://doi.org/10.1021/acssuschemeng.1c05587).
- 21 Y. C. Kim, *et al.*, UV-curing kinetics and performance development of in situ curable 3D printing materials, *Eur. Polym. J.*, 2017, **93**, 140–147, DOI: [10.1016/j.eurpolymj.2017.05.041](https://doi.org/10.1016/j.eurpolymj.2017.05.041).
- 22 L. Yue, *et al.*, Vitrimerization: Converting Thermoset Polymers into Vitrimers, *ACS Macro Lett.*, 2020, **9**(6), 836–842, DOI: [10.1021/acsmacrolett.0c00299](https://doi.org/10.1021/acsmacrolett.0c00299).
- 23 V. Schenk, K. Labastie, M. Destarac, P. Olivier and M. Guerre, Vitrimer composites: current status and future challenges, *Mater. Adv.*, 2022, **3**(22), 8012–8029, DOI: [10.1039/D2MA00654E](https://doi.org/10.1039/D2MA00654E).
- 24 S. Ma, T. Li, X. Liu and J. Zhu, Research progress on bio-based thermosetting resins, *Polym. Int.*, 2016, **65**(2), 164–173, DOI: [10.1002/pi.5027](https://doi.org/10.1002/pi.5027).
- 25 H. Q. Pham and M. J. Marks, Epoxy Resins, *Ullmann's Encyclopedia of Industrial Chemistry*, 1st edn, Wiley-VCH, 2005, DOI: [10.1002/14356007.a09\\_547.pub2](https://doi.org/10.1002/14356007.a09_547.pub2).
- 26 S. Grauzeliene, A. Navaruckiene, E. Skliutas, M. Malinauskas, A. Serra and J. Ostrauskaite, Vegetable Oil-Based Thiol-Ene/Thiol-Epoxy Resins for Laser Direct Writing 3D Micro-/Nano-Lithography, 2021.
- 27 R. Sekula, K. Immonen, S. Metsä-Kortelainen, M. Kuniewski, P. Zydrón and T. Kalpio, Characteristics of 3D Printed Biopolymers for Applications in High-Voltage Electrical Insulation, *Polymers*, 2023, **15**(11), 2518, DOI: [10.3390/polym15112518](https://doi.org/10.3390/polym15112518).
- 28 L. Pezzana, R. Wolff, J. Stampfl, R. Liska and M. Sangermano, High temperature vat photopolymerization 3D printing of fully bio-based composites: Green vegetable oil epoxy matrix & bio-derived filler powder, *Addit. Manuf.*, 2024, **79**, 103929, DOI: [10.1016/j.addma.2023.103929](https://doi.org/10.1016/j.addma.2023.103929).
- 29 X. Lu and X. Gu, 'A review on lignin-based epoxy resins: Lignin effects on their synthesis and properties', *Int. J. Biol. Macromol.*, 2023, **229**, 778–790, DOI: [10.1016/j.ijbiomac.2022.12.322](https://doi.org/10.1016/j.ijbiomac.2022.12.322).
- 30 F. Wang, J. Kuai, H. Pan, N. Wang and X. Zhu, 'Study on the demethylation of enzymatic hydrolysis lignin and the properties of lignin-epoxy resin blends', *Wood Sci. Technol.*, 2018, **52**(5), 1343–1357, DOI: [10.1007/s00226-018-1024-z](https://doi.org/10.1007/s00226-018-1024-z).
- 31 R. J. Li, J. Gutierrez, Y.-L. Chung, C. W. Frank, S. L. Billington and E. S. Sattely, 'A lignin-epoxy resin derived from biomass as an alternative to formaldehyde-based wood adhesives', *Green Chem.*, 2018, **20**(7), 1459–1466, DOI: [10.1039/C7GC03026F](https://doi.org/10.1039/C7GC03026F).
- 32 P. Niedermann, G. Szebényi and A. Toldy, 'Characterization of high glass transition temperature sugar-based epoxy resin composites with jute and carbon fibre reinforcement', *Compos. Sci. Technol.*, 2015, **117**, 62–68, DOI: [10.1016/j.compscitech.2015.06.001](https://doi.org/10.1016/j.compscitech.2015.06.001).
- 33 N. Eid, B. Ameduri and B. Boutevin, 'Synthesis and Properties of Furan Derivatives for Epoxy Resins', *ACS Sustainable Chem. Eng.*, 2021, **9**(24), 8018–8031, DOI: [10.1021/acssuschemeng.0c09313](https://doi.org/10.1021/acssuschemeng.0c09313).
- 34 L. Pezzana, *et al.*, Hot-lithography 3D printing of biobased epoxy resins', *Polymer*, 2022, **254**, 125097, DOI: [10.1016/j.polymer.2022.125097](https://doi.org/10.1016/j.polymer.2022.125097).
- 35 M. Shibata, S. Yoshihara, M. Yashiro and Y. Ohno, Thermal and mechanical properties of sorbitol-based epoxy resin cured with quercetin and the biocomposites with wood flour, *J. Appl. Polym. Sci.*, 2013, **128**(5), 2753–2758, DOI: [10.1002/app.38438](https://doi.org/10.1002/app.38438).
- 36 A. M. Atta, R. Mansour, M. I. Abdou and A. M. Sayed, 'Epoxy resins from rosin acids: synthesis and characterization', *Polym. Adv. Tech.*, 2004, **15**(9), 514–522, DOI: [10.1002/pat.507](https://doi.org/10.1002/pat.507).
- 37 A. M. Atta, R. Mansour, M. I. Abdou and A. M. El-Sayed, 'Synthesis and Characterization of Tetra-Functional Epoxy Resins from Rosin', *J. Polym. Res.*, 2005, **12**(2), 127–138, DOI: [10.1007/s10965-004-2936-x](https://doi.org/10.1007/s10965-004-2936-x).
- 38 S. Benyahya, C. Aouf, S. Caillol, B. Boutevin, J. P. Pascault and H. Fulcrand, 'Functionalized green tea tannins as phenolic prepolymers for bio-based epoxy resins', *Ind. Crops Prod.*, 2014, **53**, 296–307, DOI: [10.1016/j.indcrop.2013.12.045](https://doi.org/10.1016/j.indcrop.2013.12.045).
- 39 S. Kumar, S. K. Samal, S. Mohanty and S. K. Nayak, Recent Development of Biobased Epoxy Resins: A Review, *Polym.-Plast. Technol. Eng.*, 2018, **57**(3), 133–155, DOI: [10.1080/03602559.2016.1253742](https://doi.org/10.1080/03602559.2016.1253742).
- 40 F. Ferdosian, Y. Zhang, Z. Yuan, M. Anderson and C. (Charles) Xu, 'Curing kinetics and mechanical properties of bio-based epoxy composites comprising lignin-based epoxy resins', *Eur. Polym. J.*, 2016, **82**, 153–165, DOI: [10.1016/j.eurpolymj.2016.07.014](https://doi.org/10.1016/j.eurpolymj.2016.07.014).
- 41 E. A. Baroncini, S. Kumar Yadav, G. R. Palmese and J. F. Stanzione, 'Recent advances in bio-based epoxy resins and



- bio-based epoxy curing agents', *J. Appl. Polym. Sci.*, 2016, **133**(45), 44103, DOI: [10.1002/app.44103](https://doi.org/10.1002/app.44103).
- 42 R. Mustapha, A. R. Rahmat, R. Abdul Majid and S. N. H. Mustapha, 'Vegetable oil-based epoxy resins and their composites with bio-based hardener: a short review', *Polym.-Plast. Technol. Mater.*, 2019, **58**(12), 1311–1326, DOI: [10.1080/25740881.2018.1563119](https://doi.org/10.1080/25740881.2018.1563119).
- 43 C. Veith, F. Diot-Néant, S. A. Miller and F. Allais, 'Synthesis and polymerization of bio-based acrylates: a review', *Polym. Chem.*, 2020, **11**(47), 7452–7470, DOI: [10.1039/D0PY01222J](https://doi.org/10.1039/D0PY01222J).
- 44 J. T. Sutton, K. Rajan, D. P. Harper and S. C. Chmely, Lignin-containing photoactive resins for 3D printing by stereolithography, 2018.
- 45 R. M. Johnson, K. P. Cortés-Guzmán, S. D. Perera, A. R. Parikh, W. E. Voit and R. A. Smaldone, Lignin-Based Covalent Adaptable Network Resins for Digital Light Projection 3D Printing, 2023.
- 46 R. Ding, Y. Du, R. B. Goncalves, L. F. Francis and T. M. Reineke, 'Sustainable near UV-curable acrylates based on natural phenolics for stereolithography 3D printing', *Polym. Chem.*, 2019, **10**(9), 1067–1077, DOI: [10.1039/C8PY01652F](https://doi.org/10.1039/C8PY01652F).
- 47 A. W. Bassett, A. E. Honnig, C. M. Breyta, I. C. Dunn, J. J. La Scala and J. F. Stanzione, 'Vanillin-Based Resin for Additive Manufacturing', *ACS Sustainable Chem. Eng.*, 2020, **8**(14), 5626–5635, DOI: [10.1021/acssuschemeng.0c00159](https://doi.org/10.1021/acssuschemeng.0c00159).
- 48 K. P. Cortés-Guzmán, A. R. Parikh, M. L. Sparacin, M. Ecker, W. E. Voit and R. A. Smaldone, Thermal Annealing Effects on the Mechanical Properties of Bio-based 3D Printed Thermosets, 2023.
- 49 A. Liguori, K. I. Garfias González and M. Hakkarainen, 'Unexpected self-assembly of carbon dots during digital light processing 3D printing of vanillin Schiff-base resin', *Polymer*, 2023, **283**, 126252, DOI: [10.1016/j.polymer.2023.126252](https://doi.org/10.1016/j.polymer.2023.126252).
- 50 S. Grauzeliene, A.-S. Schuller, C. Delaite and J. Ostrauskaite, 'Development and Digital Light Processing 3D Printing of a Vitriimer Composed of Glycerol 1,3-Diglycerolate Diacrylate and Tetrahydrofurfuryl Methacrylate', *ACS Appl. Polym. Mater.*, 2023, **5**(9), 6958–6965, DOI: [10.1021/acsapm.3c01018](https://doi.org/10.1021/acsapm.3c01018).
- 51 J. Guit, *et al.*, Photopolymer Resins with Biobased Methacrylates Based on Soybean Oil for Stereolithography', *ACS Appl. Polym. Mater.*, 2020, **2**(2), 949–957, DOI: [10.1021/acsapm.9b01143](https://doi.org/10.1021/acsapm.9b01143).
- 52 B. Sölle, U. Shaukat, E. Rossegger and S. Schlögl, 'Synthesis and characterization of bio-based transesterification catalysts for green 3D-printable dynamic photopolymers', *Polym. Chem.*, 2023, **14**(44), 4994–5003, DOI: [10.1039/D3PY00989K](https://doi.org/10.1039/D3PY00989K).
- 53 Y. Wu, C. Li, T. Chen, R. Qiu and W. Liu, 'Photo-curing 3D printing of micro-scale bamboo fibers reinforced palm oil-based thermosets composites', *Composites, Part A*, 2022, **152**, 106676, DOI: [10.1016/j.compositesa.2021.106676](https://doi.org/10.1016/j.compositesa.2021.106676).
- 54 Y. Zeng, D. Sha, L. Zhang, Y. Chen, R. Qiu and W. Liu, 'Photo-Curing 3D Printing of Highly Deformable Palm Oil-Based Thermosets with Soft Fatty Acid Chain Entanglement', *ACS Sustainable Chem. Eng.*, 2023, **11**(9), 3780–3788, DOI: [10.1021/acssuschemeng.2c06932](https://doi.org/10.1021/acssuschemeng.2c06932).
- 55 V. Schimpf, A. Asmacher, A. Fuchs, K. Stoll, B. Bruchmann and R. Mülhaupt, 'Low-Viscosity Limonene Dimethacrylate as a Bio-Based Alternative to Bisphenol A-Based Acrylic Monomers for Photocurable Thermosets and 3D Printing', *Macro Mater. Eng.*, 2020, **305**(8), 2000210, DOI: [10.1002/mame.202000210](https://doi.org/10.1002/mame.202000210).
- 56 P. S. Klee, C. Vazquez-Martel, L. Florido Martins and E. Blasco, 'Designing Sustainable Polymers: Lactate Esters for 3D Printing and Upcycling', *ACS Appl. Polym. Mater.*, 2024, **6**(1), 935–942, DOI: [10.1021/acsapm.3c02497](https://doi.org/10.1021/acsapm.3c02497).
- 57 L. Pezzana, *et al.*, DLP 3D printing of levoglucosenone-based monomers: exploiting thiol-ene chemistry for bio-based polymeric resins, *ChemSusChem*, 2024, e202301828, DOI: [10.1002/cssc.202301828](https://doi.org/10.1002/cssc.202301828).
- 58 A. B. Lowe, 'Thiol-ene "click" reactions and recent applications in polymer and materials synthesis: a first update', *Polym. Chem.*, 2014, **5**(17), 4820–4870, DOI: [10.1039/C4PY00339J](https://doi.org/10.1039/C4PY00339J).
- 59 E. Constant, O. King and A. C. Weems, 'Bioderived 4D Printable Terpene Photopolymers from Limonene and  $\beta$ -Myrcene', *Biomacromolecules*, 2022, **23**(6), 2342–2352, DOI: [10.1021/acs.biomac.2c00085](https://doi.org/10.1021/acs.biomac.2c00085).
- 60 D. P. Nair, N. B. Cramer, T. F. Scott, C. N. Bowman and R. Shandas, 'Photopolymerized thiol-ene systems as shape memory polymers', *Polymer*, 2010, **51**(19), 4383–4389, DOI: [10.1016/j.polymer.2010.07.027](https://doi.org/10.1016/j.polymer.2010.07.027).
- 61 M. K. Stanfield, N. Kotlarewski, J. Smith and S. C. Thickett, 'Biobased Transparent Thiol-Ene Polymer Networks from Levoglucosan', *ACS Appl. Polym. Mater.*, 2024, **6**(1), 837–845, DOI: [10.1021/acsapm.3c02450](https://doi.org/10.1021/acsapm.3c02450).
- 62 L. Papadopoulos, L. Pezzana, N. M. Malitowski, M. Sangermano, D. N. Bikiaris and T. Robert, 'UV-Curing Additive Manufacturing of Bio-Based Thermosets: Effect of Diluent Concentration on Printing and Material Properties of Itaconic Acid-Based Materials', *ACS Omega*, 2023, **8**(34), 31009–31020, DOI: [10.1021/acsomega.3c02808](https://doi.org/10.1021/acsomega.3c02808).
- 63 J. McDonald-Wharry, M. Amirpour, K. L. Pickering, M. Battley and Y. Fu, 'Moisture sensitivity and compressive performance of 3D-printed cellulose-biopolyester foam lattices', *Addit. Manuf.*, 2021, **40**, 101918, DOI: [10.1016/j.addma.2021.101918](https://doi.org/10.1016/j.addma.2021.101918).
- 64 M. Maturi, *et al.*, Meth)acrylate-Free Three-Dimensional Printing of Bio-Derived Photocurable Resins with Terpene- and Itaconic Acid-Derived Poly(ester-thioether)s', *ACS Sustainable Chem. Eng.*, 2023, **11**(49), 17285–17298, DOI: [10.1021/acssuschemeng.3c04576](https://doi.org/10.1021/acssuschemeng.3c04576).
- 65 K. Bouzidi, D. Chaussy, A. Gandini, E. Flahaut, R. Bongiovanni and D. Beneventi, 'Bio-based formulation of an electrically conductive ink with high potential for additive manufacturing by direct ink writing', *Compos. Sci. Technol.*, 2022, **230**, 109765, DOI: [10.1016/j.compscitech.2022.109765](https://doi.org/10.1016/j.compscitech.2022.109765).
- 66 S. Gu, Y. Tian, K. Liang and Y. Ji, 'Chitin nanocrystals assisted 3D printing of polycitrate thermoset bioelastomers', *Carbohydr. Polym.*, 2021, **256**, 117549, DOI: [10.1016/j.carbpol.2020.117549](https://doi.org/10.1016/j.carbpol.2020.117549).



- 67 P. R. Sarika, P. Nancarrow, A. Khansaheb and T. Ibrahim, 'Bio-Based Alternatives to Phenol and Formaldehyde for the Production of Resins', *Polymers*, 2020, **12**(10), 2237, DOI: [10.3390/polym12102237](https://doi.org/10.3390/polym12102237).
- 68 X. Liu, Y. Hu, L. Hu, M. Zhang, P. Jia and Y. Zhou, 'Recent progress in bio-based light-curable resins used for 3D printing: From synthetic strategies to structural properties and resin applications', *React. Funct. Polym.*, 2025, **215**, 106359, DOI: [10.1016/j.reactfunctpolym.2025.106359](https://doi.org/10.1016/j.reactfunctpolym.2025.106359).
- 69 A. C. Weems, K. R. Delle Chiaie, J. C. Worch, C. J. Stubbs and A. P. Dove, 'Terpene- and terpenoid-based polymeric resins for stereolithography 3D printing', *Polym. Chem.*, 2019, **10**(44), 5959–5966, DOI: [10.1039/C9PY00950G](https://doi.org/10.1039/C9PY00950G).
- 70 A. L. Flourat, *et al.*, Levoglucosenone to 3D-printed green materials: synthesizing sustainable and tunable monomers for eco-friendly photo-curing', *Green Chem.*, 2023, **25**(19), 7571–7581, DOI: [10.1039/D3GC01833D](https://doi.org/10.1039/D3GC01833D).
- 71 J. Yao and M. Hakkarainen, 'Methacrylated wood flour-reinforced "all-wood" derived resin for digital light processing (DLP) 3D printing', *Compos. Commun.*, 2023, **38**, 101506, DOI: [10.1016/j.coco.2023.101506](https://doi.org/10.1016/j.coco.2023.101506).
- 72 Y. Hu, *et al.*, A green and sustainable strategy for recyclable ultraviolet (UV)-curable resin from tartaric acid via three dimensional (3D) printing to reduce plastic pollution', *J. Cleaner Prod.*, 2024, **436**, 140772, DOI: [10.1016/j.jclepro.2024.140772](https://doi.org/10.1016/j.jclepro.2024.140772).
- 73 M. John and S. Thomas, 'Biofibres and biocomposites', *Carbohydr. Polym.*, 2008, **71**(3), 343–364, DOI: [10.1016/j.carbpol.2007.05.040](https://doi.org/10.1016/j.carbpol.2007.05.040).
- 74 T. H. Mokhothu, M. J. John and M. J. John, Bio-Based Fillers for Environmentally Friendly Composites, in *Handbook of Composites from Renewable Materials*, ed. V. K. Thakur, M. K. Thakur, and M. R. Kessler, Wiley, 2017, 1st edn, pp. 243–270, DOI: [10.1002/9781119441632.ch10](https://doi.org/10.1002/9781119441632.ch10).
- 75 K. Pitt, O. Lopez-Botello, A. D. Lafferty, I. Todd and K. Mumtaz, 'Investigation into the material properties of wooden composite structures with in-situ fibre reinforcement using additive manufacturing', *Compos. Sci. Technol.*, 2017, **138**, 32–39, DOI: [10.1016/j.compscitech.2016.11.008](https://doi.org/10.1016/j.compscitech.2016.11.008).
- 76 M. Kariz, M. Sernek and M. K. Kuzman, 'Use of wood powder and adhesive as a mixture for 3D printing', *Eur. J. Wood Prod.*, 2016, **74**(1), 123–126, DOI: [10.1007/s00107-015-0987-9](https://doi.org/10.1007/s00107-015-0987-9).
- 77 S. Kumar, M. Hofmann, B. Steinmann, E. J. Foster and C. Weder, 'Reinforcement of Stereolithographic Resins for Rapid Prototyping with Cellulose Nanocrystals', *ACS Appl. Mater. Interfaces*, 2012, **4**(10), 5399–5407, DOI: [10.1021/am301321v](https://doi.org/10.1021/am301321v).
- 78 F. M. Khan, *et al.*, A Comprehensive Review on Epoxy Biocomposites Based on Natural Fibers and Bio-fillers: Challenges, Recent Developments and Applications', *Adv. Fiber Mater.*, 2022, **4**(4), 683–704, DOI: [10.1007/s42765-022-00143-w](https://doi.org/10.1007/s42765-022-00143-w).
- 79 V. Mazzanti, L. Malagutti and F. Mollica, 'FDM 3D Printing of Polymers Containing Natural Fillers: A Review of their Mechanical Properties', *Polymers*, 2019, **11**(7), 1094, DOI: [10.3390/polym11071094](https://doi.org/10.3390/polym11071094).
- 80 B. Tisserat, Z. Liu, V. Finkenstadt, B. Lewandowski, S. Ott and L. Reifschneider, '3D printing biocomposites', *SPE Plast. Res. Online*, 2015, DOI: [10.2417/spepro.005690](https://doi.org/10.2417/spepro.005690).
- 81 P. Wei, C. Cipriani, C.-M. Hsieh, K. Kamani, S. Rogers and E. Pentzer, 'Go with the flow: Rheological requirements for direct ink write printability', *J. Appl. Phys.*, 2023, **134**(10), 100701, DOI: [10.1063/5.0155896](https://doi.org/10.1063/5.0155896).
- 82 E. Morici and N. T. Dintcheva, 'Recycling of Thermoset Materials and Thermoset-Based Composites: Challenge and Opportunity', *Polymers*, 2022, **14**(19), 4153, DOI: [10.3390/polym14194153](https://doi.org/10.3390/polym14194153).
- 83 A. K. Das, D. A. Agar, M. Rudolfsson and S. H. Larsson, 'A review on wood powders in 3D printing: processes, properties and potential applications', *J. Mater. Res. Technol.*, 2021, **15**, 241–255, DOI: [10.1016/j.jmrt.2021.07.110](https://doi.org/10.1016/j.jmrt.2021.07.110).
- 84 U. Bodenschatz and M. Rosenthal, '3D printing of a wood-based furniture element with liquid deposition modeling', *Eur. J. Wood Prod.*, 2024, **82**(1), 241–244, DOI: [10.1007/s00107-023-01996-7](https://doi.org/10.1007/s00107-023-01996-7).
- 85 Z. Zeng, Y. Zhou, S. Wen and C. Zhou, 'A review: additive manufacturing of wood-plastic composites', *Cellulose*, 2024, **31**(9), 5315–5341, DOI: [10.1007/s10570-024-05916-7](https://doi.org/10.1007/s10570-024-05916-7).
- 86 M. Hubbe and W. Grigsby, 'From nanocellulose to wood particles: A review of particle size vs. the properties of plastic composites reinforced with cellulose-based entities', *BioRes*, 2020, **15**(1), 2030–2081.
- 87 N. B. Palaganas, J. O. Palaganas, S. H. Z. Doroteo and J. C. Millare, 'Covalently functionalized cellulose nanocrystal-reinforced photocurable thermosetting elastomer for 3D printing application', *Addit. Manuf.*, 2023, **61**, 103295, DOI: [10.1016/j.addma.2022.103295](https://doi.org/10.1016/j.addma.2022.103295).
- 88 A. Babaei-Ghazvini, B. Vafakish, R. Patel, K. J. Falua, M. J. Dunlop and B. Acharya, 'Cellulose nanocrystals in the development of biodegradable materials: A review on CNC resources, modification, and their hybridization', *Int. J. Biol. Macromol.*, 2024, **258**, 128834, DOI: [10.1016/j.ijbiomac.2023.128834](https://doi.org/10.1016/j.ijbiomac.2023.128834).
- 89 S. Kumar, M. Hofmann, B. Steinmann, E. J. Foster and C. Weder, 'Reinforcement of Stereolithographic Resins for Rapid Prototyping with Cellulose Nanocrystals', *ACS Appl. Mater. Interfaces*, 2012, **4**(10), 5399–5407, DOI: [10.1021/am301321v](https://doi.org/10.1021/am301321v).
- 90 K. Peng, *et al.*, Microporous polylactic acid/chitin nanocrystals composite scaffolds using in-situ foaming 3D printing for bone tissue engineering', *Int. J. Biol. Macromol.*, 2024, **279**, 135055, DOI: [10.1016/j.ijbiomac.2024.135055](https://doi.org/10.1016/j.ijbiomac.2024.135055).
- 91 A. Alhelal, Z. Mohammed, S. Jeelani and V. K. Rangari, '3D printing of spent coffee ground derived biochar reinforced epoxy composites', *J. Compos. Mater.*, 2021, **55**(25), 3651–3660, DOI: [10.1177/00219983211002237](https://doi.org/10.1177/00219983211002237).
- 92 V. C.-F. Li, C. K. Dunn, Z. Zhang, Y. Deng and H. J. Qi, 'Direct Ink Write (DIW) 3D Printed Cellulose Nanocrystal Aerogel Structures', *Sci. Rep.*, 2017, DOI: [10.1038/s41598-017-07771-y](https://doi.org/10.1038/s41598-017-07771-y).
- 93 S. Gu, Y. Tian, K. Liang and Y. Ji, 'Chitin nanocrystals assisted 3D printing of polycitrate thermoset bioelastomers', *Carbohydr. Polym.*, 2021, **256**, 117549, DOI: [10.1016/j.carbpol.2020.117549](https://doi.org/10.1016/j.carbpol.2020.117549).

